

SBUF 13225: Process and quality control of grouting
Doctoral student: John Shamu ^a
Supervisors: Ulf Håkansson ^{a,b} and Stefan Larsson ^a
^a KTH Royal Institute of Technology, ^b Skanska Sweden AB ^b

Abstract

The rheological (flow) properties of cement-based grouts play a key role in determining the final spread in grouted rock formations. Rheologically, cement grouts are known to be complex thixotropic fluids, but their behavior is often described by fitting the simple Bingham constitutive model to flow curve data. The resultant Bingham parameters are then used in grouting design of e.g. tunnels, to estimate the penetration length. Due to their thixotropic nature, the interpretation of cement grout flow curves is often complicated by: the presence of wall slip, sedimentation and unstable flow at low shear rates (particularly below the critical shear rate). A systematic approach to study these effects within the constraints of different concentric cylinder geometries (Couette), measurement interval and for typical cement grout mixes (w/c 0.6-0.8) was carried out. The results showed that depending on rheometer geometry and measurement interval: (1) in general for cement grouts, there exists a critical shear rate related to the yield stress below which no stable flow occurs, (2) severe wall slip in certain Couette geometries and (3) sedimentation effects especially in the vane geometry, that need to be accounted for in flow curve analyses. Following this, some suggestions were made towards the development of a well-defined cement grout flow curve measurement and Bingham fitting protocol.

Additionally, as part of the research work; a 2D radial flow model for understanding fundamental grout spread in planar rock fractures was designed, manufactured and tested. The importance of the work was in visualizing 2D radial flow velocity profiles of a model yield stress fluid (YSF), whilst using ultrasound velocimetry for apparently the first time. The model YSF used was Carbopol in place of actual cement grouts that would otherwise show complex time dependent behavior during the time frame of the experiments. The current observations for tests carried out with different apertures (disk spacings) and injection flow rates show that indeed a distinct plug region in 2D radial flow exists. As expected, in the case of smooth plexiglass disks used, significant wall slip effects were noted by non-zero wall velocities in the measured velocity profiles. This experimental work was thus a first step towards more systematic studies on the plug flow region and verifying analytical solutions that are currently used for estimating grout spread in radial flows.

1 Introduction

Cement-based grouting is an essential component of large infrastructure projects around Sweden e.g. in tunneling and dam constructions [1]–[3]. The widespread use of cementitious materials for grouting is mainly due to their relatively low cost and the fact that they pose less of a risk to the environment compared to chemical based grouts [4]. The environmental court ruling stipulating limited water ingress into underground tunnels has become stricter in recent years in an attempt to mitigate consequential environmental impacts e.g. settlements and drainage of water resources [5]. These stricter regulations, combined with the need to reduce grouting time and costs has led to focused grouting research aimed at improving the cement grouts' flow properties and their measurement in relation to the actual grouting application.

The current state of research related to cement grout flow properties has now reached an advanced level, at which new digital technologies for quality monitoring e.g. ultrasound based rheological measurements are now being tested and optimized for the improvement of grouting applications [6], [7]. Ideally the goal is to measure the rheological properties during the grouting process (*inline*, Figure 1c) for quality monitoring and control, and reduce *offline* methods and the use of unreliable devices e.g. marsh cones in actual field applications (Figure 1a). Simple devices such as marsh funnels only offer the approximate viscosity at a single shear rate (flow rate) as opposed to the entire flow curve (see Figure 1b). From a fundamental standpoint, there is still a lot of work to be done in understanding the underlying phenomena that complicate the flow of cement grouts. By

understanding these phenomena grout flow can be characterized more effectively, enabling the proper implementation of inline methods and overall improvements in grouting design and execution.

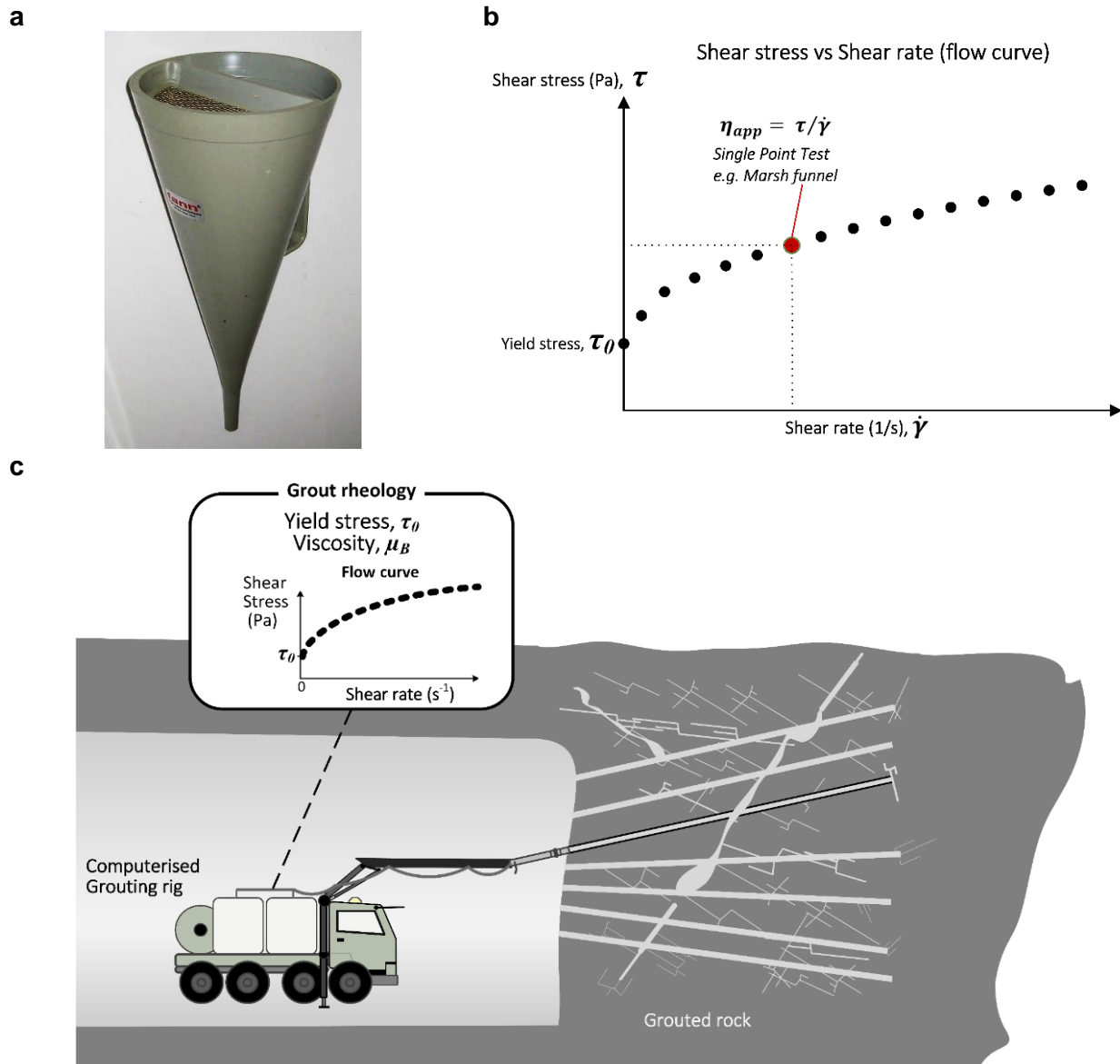


Figure 1: (a) Image of a marsh funnel (b) Flow curve schematic (c) illustration of inline monitoring of cement grout rheology, close to the injection point.

To measure these rheological properties in a controlled way, rotational rheometry tests are often carried out (offline method). For these tests, rheometers are used in either controlled shear rate (CSR) or controlled shear stress (CSS) mode for flow sweeps to obtain a flow curve (shear stress-shear rate relationship of the cement grout, Figure 1b). The resultant flow curve data from rotational tests is often fitted with the Bingham constitutive law, which is a simplified model often used to describe the flow behavior of yield stress fluids (YSF). The Bingham model is described as: $\tau = \tau_0^B + \mu_B \dot{\gamma}$, where the yield stress is τ_0^B , the Bingham (plastic) viscosity is μ_B , τ is the shear stress and $\dot{\gamma}$ the shear rate. However, this model simplification does not take into account flow phenomena such as: (1) *flow localization* in the form of shear banding and shear localization, (2) wall slip and (3) sedimentation that are inherent in the rheological testing of suspensions such as cement grouts.

Flow localization is when the fluid in the flow geometry separates into flowing and non-flowing layers in the lower shear rate ranges. Specifically, shear banding is flow localization that is linked to the inherent physical material properties of thixotropic suspensions e.g. cement grouts, laponite and drilling muds, that cannot flow below the yield stress and an associated *critical shear rate* $\dot{\gamma}_c$; whereas shear localization is separation into static and flowing bands due to flow geometry i.e. when the yield stress τ_0 , is not surpassed throughout the entire shear gap [8]. Wall slip, sedimentation and secondary flow are characteristic properties of suspensions that are in turn influenced by rheometer geometry and measurement interval t_w . Within grouting literature there had not been much research work detailing the combined influence of rheometer geometry, measurement interval on the critical shear rate and wall slip phenomena as seen in the flow curves of cement grouts, especially at low shear rates (< 10 1/s). In order to get a detailed understanding of such unstable flow behavior, a systematic study consisting of different rotational rheometric tests was carried out on typical cement grouts. The results showed that for typical cement grouts there exists regions in the flow curve that are dominated by unstable flow below a critical shear rate and wall slip that need to be taken into account during the analysis of flow curves.

Furthermore, and related to grout spread estimation is the radial flow configuration in which a YSF flows between smooth parallel plates. Such a fundamental flow configuration in which a fluid penetrates the center of two disks is of interest to applications such as rock grouting design, since it ideally simulates cement grouts propagation from a central injection borehole, from where they spread radially outward into surrounding fractures [4], [9] (Figure 2). The plug flow region of the velocity profile of a YSF is directly related to the yield stress property τ_0 of the fluid, since the plug region is an unsheared region, wherein the fluid stresses across the aperture are below the yield stress. Only a limited amount of works have presented analytical and numerical solutions describing the expected velocity profiles for YSFs in this flow geometry [5], [10], [11]. Thus, an experimental study as a first step towards verifying existing theory, based on the lubrication approximation, together with the measurement of the shape of the plug flow region across the radial length also formed a major part of the current research work.

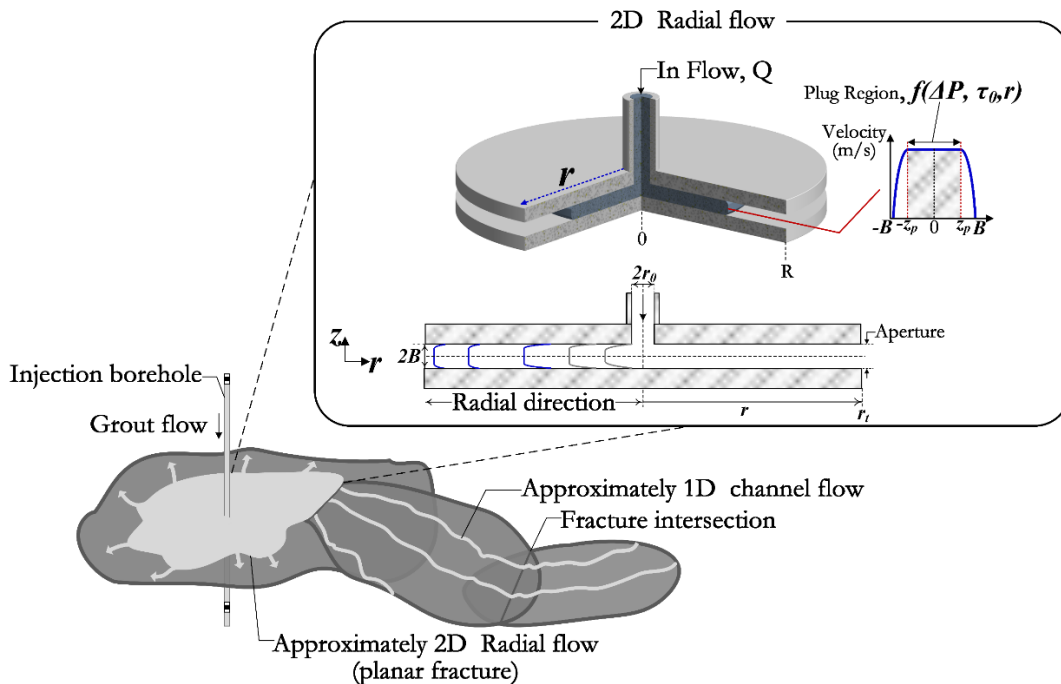


Figure 2: Schematic illustrating the idealized 1D channel and 2D radial flow configurations

2 Experimental Methods

2.1 Cement grout flow curve measurements

Three different concentric cylinder geometries were used in the systematic study of flow curves obtained from typical cement grouts prepared at water to cement (w/c) ratios of 0.6 and 0.8. The grouts were prepared from Cements Injektering 30 as supplied by Cements AB, by mixing them at a high shear rate of 1000 rpm using a high shear mixer for ~4 minutes. No additives were used in order to study the behavior of the pure cement. About ~2 minutes after mixing the cement grouts were then loaded into the rheometer geometry and presheared at 300 1/s to achieve a reference point for measurements that is free from different sample loading stresses. The entire mixing and measurement procedure is described by [8].

Flow curves were then acquired in controlled shear rate (CSR) mode at three different measurement intervals of $t_w = 4$ s; $t_w = 24$ s and $t_w = 40$ s. The measurement interval t_w being defined as the sample period or constant time where the shear rate $\dot{\gamma}$ is held constant before the corresponding shear stress is acquired. Figure 3 shows the different rheometer geometries that were used.

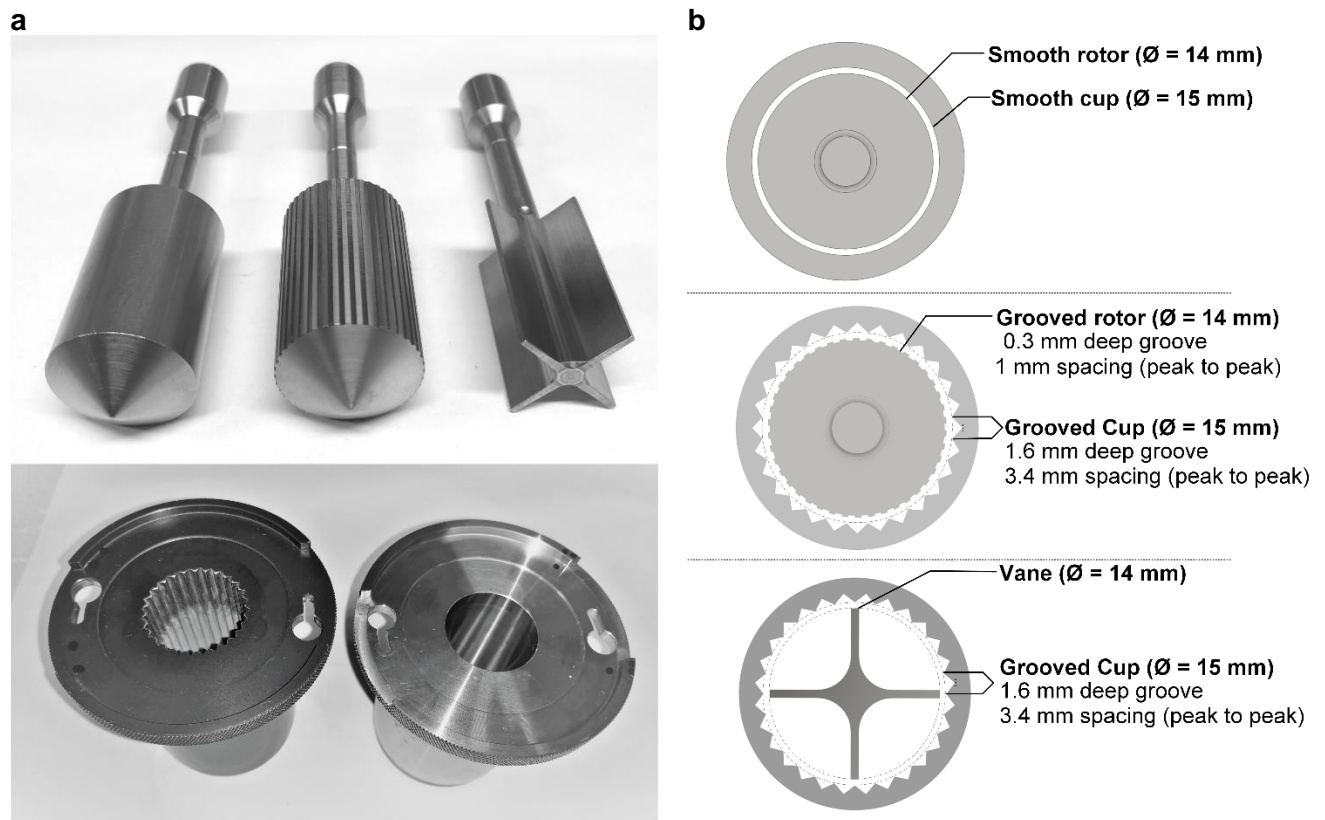


Figure 3: Rheometer geometry (a) *top row from left*, 14 mm diameter standard DIN rotor (smooth), 14 mm diameter grooved rotor and 14 mm diameter four-blade vane; *bottom row from left* grooved cup and smooth cup. Combined geometries (b) *top to bottom* smooth cup and smooth rotor, grooved rotor and grooved cup, and vane and grooved cup.

2.2 Radial flow experiments and Ultrasound Velocity Profiling (UVP)

The initial design of the physical radial model was based on earlier models presented in the literature [12], [13]. The aim was to have a radial flow area that was clear of intrusive objects e.g. fasteners, in order to clearly study the underlying radial flow of Carbopol. The entire setup including an image of the actual model used is shown in Figure 4. The system components included a magnetic flow meter (Discomag DMI 6531, Endress + Hauser) at the pump outlet and a PT100 temperature transducer.

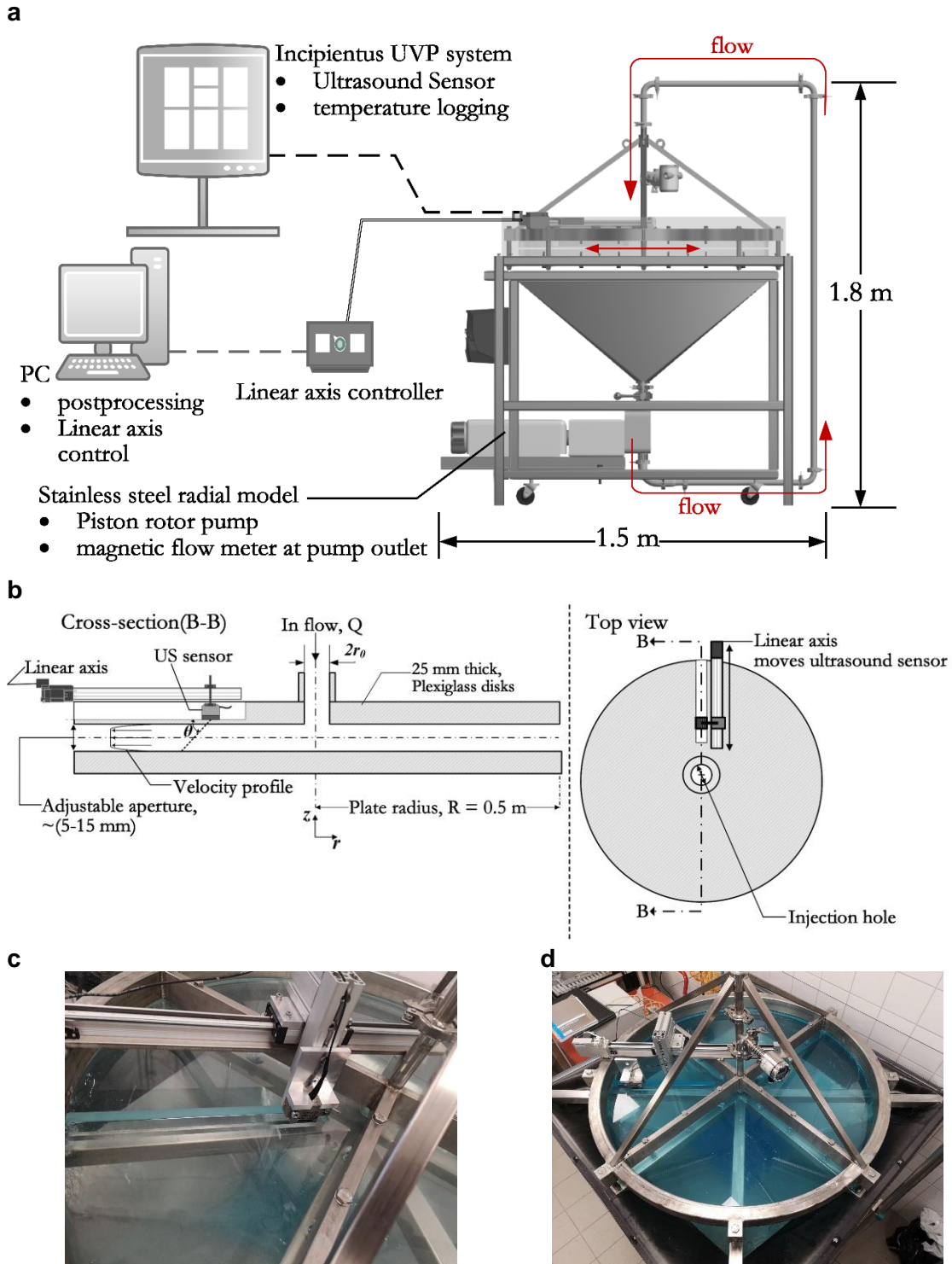


Figure 4: Radial flow model (a) schematic of the radial flow system (b) schematic of flow area between parallel plates and linear axis setup (c) image showing ultrasound sensor in slot (d) top view image of spoke frame

A piston rotor pump was used to pump the fluid at set flow rates controlled from a variable speed drive (VSD). The fluid then circulated from the bottom of the tank into the radial flow area where measurement was carried out. A motorized linear axis (Isel LEZ 1) with a repeatability of $\pm 0.2\text{ mm}$ was then used to move the ultrasound sensor (US sensor Figure 4b) used for velocimetry, to different radial locations. Schematics and images of the linear axis-slot

setup and the radial model are shown in Figure 4. The slot shown in Figure 4b and 4c was machined on the top disk to allow sufficient propagation of the ultrasound beam, without significant attenuation. After machining the wall thickness in the slot was 5 mm (originally 25 mm thick). The desired gap (aperture) was achieved by a metallic spacer system around the periphery of the disks. The top spoke frame was used as a support for the top disk, to maintain the set aperture even during high flow and pressure conditions.

2.3 Carbopol Yield Stress fluid

A yield stress model fluid Carbopol 980 (Lubrizol®, Belgium) was used for the study in place of actual cements in order to study the yield stress fluid behavior without the thixotropic and hydration effects that are characteristic of cements. The Carbopol gel was prepared according to [14], [15] with additional blue colorant and tracer particles to facilitate ultrasound velocimetry. The rheological parameters that were representative of the Carbopol gels used as taken from the flow curves were: Herschel Bulkley parameters $\tau_0 = 2.24$ Pa, $k = 2.28$ Pa.sⁿ and $n = 0.4$ (see [16]).

2.4 Ultrasound Velocity Profiling (UVP)

The UVP method used to measure velocity profiles, is a velocimetry method that has been used in a wide range of complex fluids, ranging from food products to mineral suspensions [7], [17]. The individual velocities v_i at each point of the flow geometry where the velocity profile is measured are calculated as, $v_i = cf_{d_i}/2f_0\cos\theta$ where f_0 is the central ultrasound transmission frequency, c is the velocity of sound, f_{d_i} the Doppler shift frequency for particles flowing at a certain distance position (gate) and θ is the Doppler angle. Several studies have shown that the accuracy of velocity estimation depends on the correct determination of the sound velocity in the fluid under study as well as the Doppler angle θ . The error contribution from incorrect angle values is quite significant, therefore, in this work the measurement of this angle was carried out in detail using a needle hydrophone setup as described by [18].

Once the correct Doppler angle and velocity of sound were determined, they were then used as input parameters to the UVP software of the Incipientus Flow Visualizer (IFV) system that was used for velocimetry within this study. The latest developments with the system have been on the ultrasound electronics and non-invasive sensors capable of measuring through industrial steel pipes [7], [18], [19] www.incipientus.com. Velocity profiles were then acquired along the length of the radial slot as shown in Figure 4b. Before each velocity profile acquisition the Carbopol gel was first circulated in the flow loop for ~2 minutes in order to have a fully homogenous fluid.

Plug Detection: As part of the work a custom CUSUM plug region detection algorithm was developed in order to estimate the relative plug region in each profile (see [16]).

3 Results

3.1 Flow curves: CSR flow sweeps in Couette geometry

Several flow effects were observed in the measured flow (down) curves, when systematic tests with 3 different geometry and 3 measurement intervals were carried out for the two cement grout mixes (w/c = 0.6; 0.8). Figure 5 highlights the major difference between flow curves from the completely smooth geometry compared to the vane geometry. The emergence of significant wall slip is seen in the measurements with the smooth rotor-cup geometry, starting at ~10 1/s (Figure 5a). With the vane geometry slip was greatly reduced, however the vane data had much higher measured stress values, particularly for longer measurement durations ($t_w = 24$ s, 40 s) and below the critical shear rate ($\dot{\gamma}_c$), where unstable flow branches are seen (decreasing part of the flow curve) (Figure 5b). The higher stress values in the vane data compared to the other flow curves was mainly due to increased structural build-up, sedimentation and possibly secondary flow with the vane. The grooved cup and grooved rotor geometry was expected to reduce slip, however this was not the case. Wall slip was also observed

for this geometry although it was slightly less when compared to the completely smooth geometry. The grooved rotor result therefore showed that a particular geometry roughness is required to significantly reduce slip in suspensions such as cement grouts.

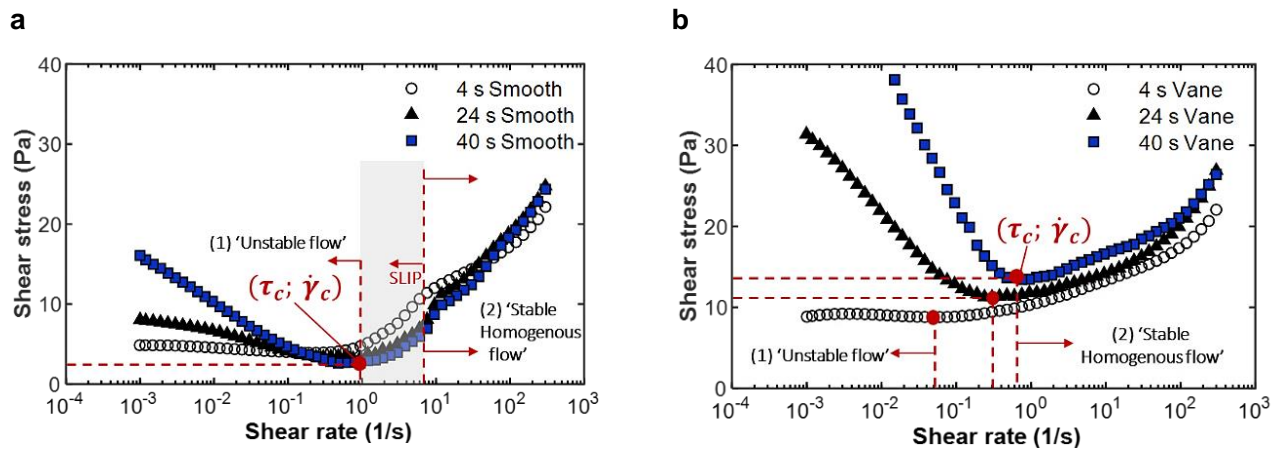


Figure 5: Flow curves of cement grouts at (w/c) of 0.6 (a) Smooth cup and smooth rotor (b) Vane and grooved cup [16]

The complete set of flow curves from all the measurements including the comparison of the Bingham fitting procedure over different shear rates is provided by [8]. Here, a simplified schematic to summarize the main findings of the flow curves study is illustrated in Figure 6. The schematic of flow curves shows that in general when the CSR based flow curves are plotted in linear-logarithmic format there is an unstable flow branch below a critical shear rate of cement grouts $\dot{\gamma}_c$. For the smoother geometries slip effects dominates till an approximate no-slip shear rate $\dot{\gamma}_{NS}$. For the cements grouts tested (w/c 0.6 and 0.8) the no-slip shear rate $\dot{\gamma}_{NS}$ reached a maximum value ~ 10 1/s and the critical shear rate $\dot{\gamma}_c$ was within ~ 0.1 -1 1/s. Hence, the data below $\dot{\gamma}_{NS}$ should also be eliminated from flow curve analysis when using completely smooth geometries.

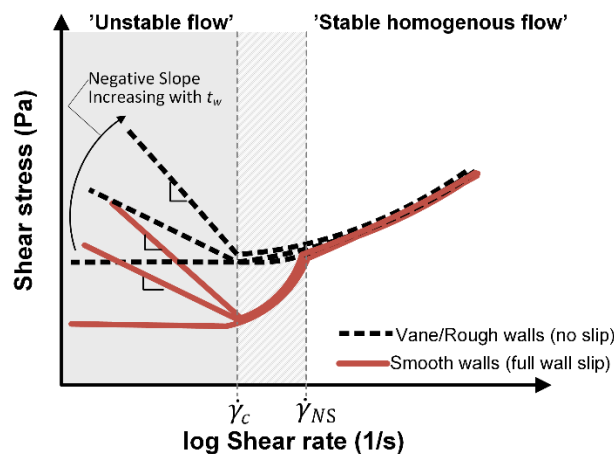


Figure 6: Generalized CSR-based flow curve schematics for typical micro cement grouts (w/c: 0.6, 08) at different measurement intervals t_w and concentric cylinder geometry

3.2 Radial flow velocity profiles

The velocity profiles measured in the radial flow model showed that for yield stress fluids a distinct plug exists in radial flow. As expected for smooth plexiglass walls, there was significant wall slip noted as non-zero wall velocities i.e. ~ 0.2 - 0.4 of the maximum axial velocity (Figure 7d,e,f). After slip correction there was relatively good agreement between the analytical determined velocity profiles and the measured ones (Figure 7b). The presence of wall slip

probably increased the overall plug length due to less shear deformation. Also, the plug flow region shape could have significantly been increased by secondary flow due to Carbopol gels' elasticity. Nevertheless, these and other related flow effects that could have been present in the radial flow data presented here need to be systematically studied and are out of the scope of the current work in this thesis.

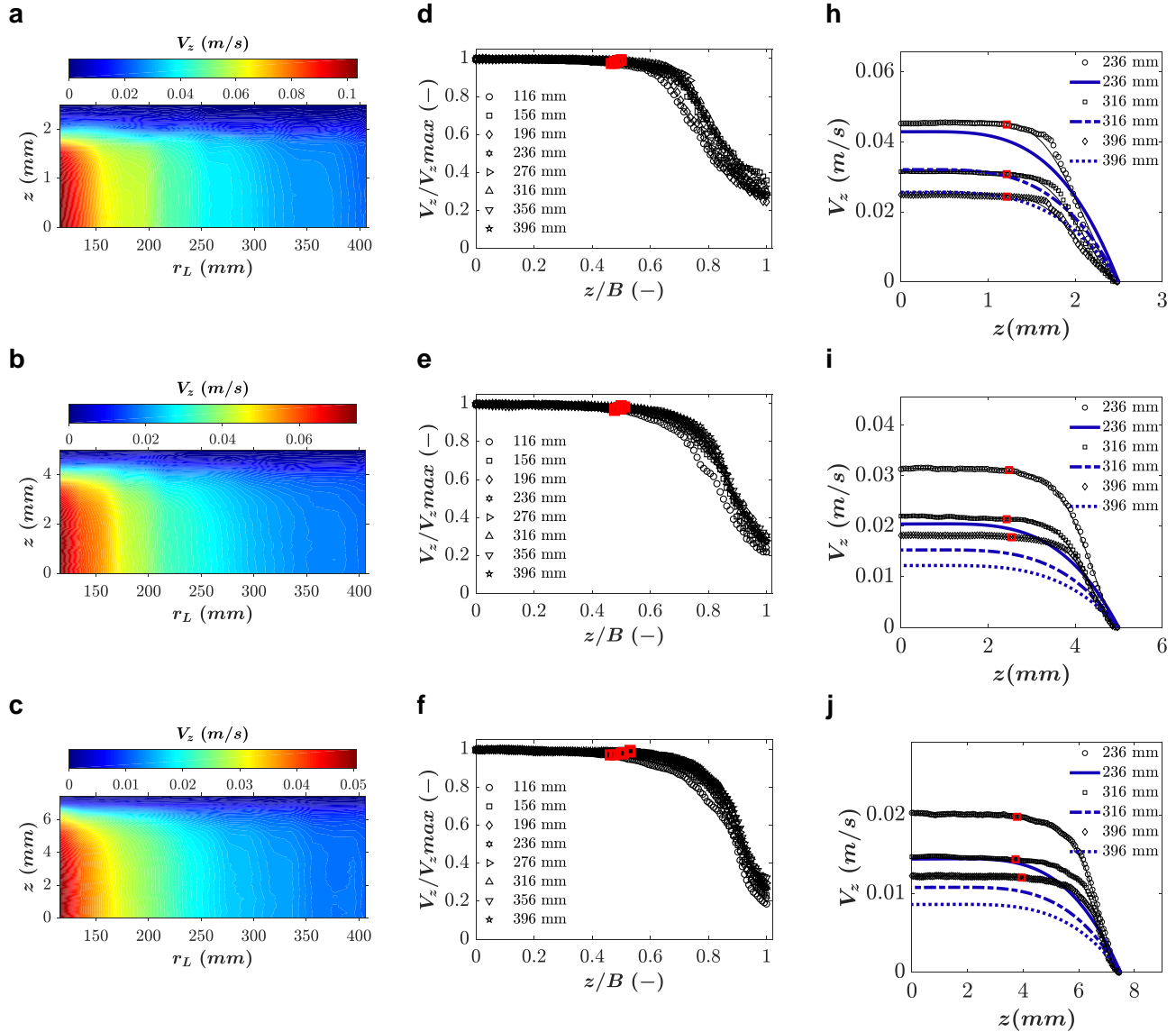


Figure 7: Contour colormaps of the velocity profiles at ~ 40 l/min, for apertures (a) 5 mm (b) 10 mm (b) 15 mm; the corresponding normalized velocity profiles (d) 5 mm (e) 10 mm (f) 15 mm, the red squares are plug region positions based on the CUSUM calculation and comparisons of analytical and measured velocity profiles at selected radial position (h) 5 mm (i) 10 mm (j) 15 mm.

4 Conclusions and Future Work

In summary, the entire work that was carried out was aimed at understanding rheological measurements related to cement-based grouts and in general YSFs, and their application to rock grouting. The main conclusions from this work, are summarized as follows:

- In general, the CSR-based flow curves of cement grouts depend on the measurement protocol including test geometry and measurement interval. The resultant flow curves can be separated into two regions: (i)

unstable flow below a critical shear rate $\dot{\gamma}_c$, where flow localization (shear localization and shear banding) is pronounced especially at longer test durations (ii) a steady homogenous shear region for shear rates above $\dot{\gamma}_c$. Wall slip effects as seen with smoother geometries below $\dot{\gamma}_{NS}$ can be eliminated by using the vane. However, the vane is more suitable for short test time since it is more susceptible to build-up, secondary flow and sedimentation.

- For radial flows, the ultrasound velocimetry was successfully used to measure the radial flow velocity profiles. The measurements showed that distinct plug regions exist, and for the length of the experimental model used the plug was relatively constant. However, the current results are not conclusive since there was some discrepancy with analytical predictions that need further investigation. These differences were explained by the presence of wall slip, insufficient entry lengths, some inaccuracies in the near wall data and the likely presence of secondary flows.
- Future, work on the measurement of cement grout rheology will focus on developing the existing inline methods for digital monitoring based on ultrasound, whilst making use of the knowledge gathered from the current offline rotational tests. As for the radial model, some adjustments to the current setup will be carried out for

5 References

- [1] U. Håkansson, "Rheology of fresh cement-based grouts," KTH Royal Institute of Technology, Stockholm, 1993.
- [2] Å. Fransson, J. Funehag, and J. Thörn, "Swedish grouting design: hydraulic testing and grout selection," *Proceedings of the Institution of Civil Engineers - Ground Improvement*, vol. 169, no. 4, pp. 275–285, Nov. 2016.
- [3] L. Zou, U. Håkansson, and V. Cvetkovic, "Two-phase cement grout propagation in homogeneous water-saturated rock fractures," *International Journal of Rock Mechanics and Mining Sciences*, vol. 106, pp. 243–249, Jun. 2018.
- [4] H. Stille, *Rock grouting - Theories and Applications*. Stockholm: Vulkanmedia, 2015.
- [5] G. Gustafson, J. Claesson, and Å. Fransson, "Steering Parameters for Rock Grouting," *Journal of Applied Mathematics*, vol. 2013, 2013.
- [6] M. Rahman, U. Håkansson, and J. Wiklund, "In-line rheological measurements of cement grouts: Effects of water/cement ratio and hydration," *Tunnelling and Underground Space Technology*, vol. 45, pp. 34–42, Jan. 2015.
- [7] M. Rahman, J. Wiklund, R. Kotzé, and U. Håkansson, "Yield stress of cement grouts," *Tunnelling and Underground Space Technology*, vol. 61, pp. 50–60, Jan. 2017.
- [8] T. J. Shamu and U. Håkansson, "Rheology of cement grouts: On the critical shear rate and no-slip regime in the Couette geometry," *Cement and Concrete Research*, p. S0008884619301437, May 2019.
- [9] U. Håkansson, "Rheology of fresh cement-based grouts," Royal Institute of Technology, Stockholm, 1993.
- [10] G. Dai and R. Byron Bird, "Radial flow of a Bingham fluid between two fixed circular disks," *Journal of Non-Newtonian Fluid Mechanics*, vol. 8, no. 3–4, pp. 349–355, Jan. 1981.
- [11] T. J. Shamu, L. Zou, R. Kotzé, J. Wiklund, and U. Håkansson, "Radial flow velocity profiles of a yield stress fluid between smooth parallel disks," Apr-2019.
- [12] S. B. Savage, "Laminar Radial Flow Between Parallel Plates," *Journal of Applied Mechanics*, vol. 31, no. 4, p. 594, 1964.
- [13] B. R. Laurencena and M. C. Williams, "Radial Flow of Non-Newtonian Fluids Between Parallel Plates," *Transactions of the Society of Rheology*, vol. 18, no. 3, pp. 331–355, Sep. 1974.
- [14] M. Dinkgreve, M. M. Denn, and D. Bonn, "'Everything flows?': elastic effects on startup flows of yield-stress fluids," *Rheologica Acta*, vol. 56, no. 3, pp. 189–194, Mar. 2017.
- [15] E. Di Giuseppe *et al.*, "Characterization of Carbopol® hydrogel rheology for experimental tectonics and geodynamics," *Tectonophysics*, vol. 642, pp. 29–45, Feb. 2015.
- [16] T. J. Shamu, "On the measurement and application of cement grout rheological properties," KTH Royal Institute of Technology, Stockholm, 2019.
- [17] J. Wiklund, I. Shahram, and M. Stading, "Methodology for in-line rheology by ultrasound Doppler velocity profiling and pressure difference techniques," *Chemical Engineering Science*, vol. 62, no. 16, pp. 4277–4293, Aug. 2007.
- [18] T. J. Shamu, R. Kotze, and J. Wiklund, "Characterization of Acoustic Beam Propagation Through High-Grade Stainless Steel Pipes for Improved Pulsed Ultrasound Velocimetry Measurements in Complex Industrial Fluids," *IEEE Sensors Journal*, vol. 16, no. 14, pp. 5636–5647, Jul. 2016.
- [19] S. Ricci, V. Meacci, B. Birkhofer, and J. Wiklund, "FPGA-Based System for In-Line Measurement of Velocity Profiles of Fluids in Industrial Pipe Flow," *IEEE Transactions on Industrial Electronics*, vol. 64, no. 5, pp. 3997–4005, May 2017.